Journal of Ovarian Research

RESEARCH

Open Access

MECOM Locus classical transcript isoforms affect tumor immune microenvironment and different targets in ovarian cancer

Ning Lan[1,2], Shuheng Bai[1], Min Chen[1,2], Xuan Wang[1], Zhaode Feng[3], Ying Gao[1], Beina Hui[1], Wen Ma[1,4], Xiangxiang Zhang[1], Fengyuan Hu[1], Wanyi Liu[1], Wenyang Li[1], Fang Wu[1] and Juan Ren[1*]

Abstract

The *MECOM* locus is a gene frequently amplified in high-grade serous ovarian carcinoma (HGSOC). Nevertheless, the body of research examining the associations among *MECOM* transcripts, patient prognosis, and their role in modulating the tumor immune microenvironment (TIME) remains sparse, particularly in large cohorts. This study assessed the expression of *MECOM* transcripts in 352 HGSOC patients and 88 normal ovarian tissues from the combined GTEx/TCGA database. Using resources such as the UCSC Genome Browser, Ensembl, and NextProt, two transcripts corresponding to classical protein isoforms from *MECOM* were identified. Cox proportional hazards regression analysis, Kaplan-Meier survival curves, and a comprehensive TIME evaluation algorithm were employed to elucidate the connections between the expression levels of these transcripts and both patient prognosis and TIME status. Chromatin Immunoprecipitation sequencing (ChIP-seq) data for the two protein isoforms, as well as RNA sequencing data post-targeted silencing, were analyzed to identify potential regulatory targets of the different transcription factors. Elevated expression of the MECOM isoform transcripts was correlated with poorer survival in HGSOC patients, potentially through the modulation of cancer-associated fibroblasts (CAFs) and immunosuppressive cell populations. In contrast, higher levels of EVI1 isoform transcripts were linked to enhanced survival, possibly due to the regulation of $CD8^+$ T cells, macrophages, and a reduction in the expression of JUN protein, or its DNA-binding activity on downstream genes. Diverse protein isoforms derived from *MECOM* were found to differentially affect the survival and tumor development in ovarian cancer patients through specific mechanisms. Investigating the molecular mechanisms underlying disease pathogenesis and identifying potential drug target proteins at the level of splice variant isoforms were deemed crucial.

Keywords Isoforms, *MECOM*, High-grade serous ovarian carcinoma (HGSOC), Regulatory targets, Transcription factors, Tumor immune microenvironment (TIME)

*Correspondence:
Juan Ren
869491533@qq.com
[1]Department of Radiotherapy, The First Affiliated Hospital of Xi'an Jiaotong University, Xi'an, Shaanxi Province 710061, PR China
[2]Precision Medicine Center, The First Affiliated Hospital of Xi'an Jiaotong University, Xi'an, Shaanxi Province 710061, PR China
[3]Center for Mitochondrial Biology and Medicine, The Key Laboratory of Biomedical Information Engineering of Ministry of Education, School of Life Science and Technology, Xi'an Jiaotong University, Xi'an, Shaanxi Province 710061, PR China
[4]Department of Radiotherapy, Gansu Provincial Hospital, Lanzhou, Gansu Province730030, PR China

Introduction

Ovarian cancer is the most lethal gynecological malignancy, with a five-year survival rate below 45%, largely due to recurrence and chemoresistance despite initial treatment involving tumor debulking surgery and platinum/paclitaxel-based chemotherapy [1]. High-grade serous ovarian carcinoma (HGSOC) is the predominant and most aggressive subtype, often associated with poor outcomes [2]. The *MECOM* locus (MDS1 and EVI1 complex locus) is amplified in over 20% of HGSOC cases and plays a pivotal role in disease progression [3]. MECOM, akin to BRCA1/2 and FOXM1, is a histotype-specific transcription factors (TF) that contributes to the pathogenesis of HGSOC [4].

The *MECOM* gene, situated at cytoband 3q26.2, exhibits a gain in 65.8-75% of HGSOC cases, as determined by spatially distinct and temporally varied tumor biopsies from individual patients [5]. *MECOM* is the general gene symbol represented by a transcriptional unit originally constituted by two main promoters (separated by 500 kb), orchestrates the production of the myelodysplastic syndrome 1 (MDS1) and ecotropic viral integration site 1 (EVI1) proteins [6]. Research indicates that *MECOM* are among the most extensively and frequently amplified transcripts among nine genes encoded within the 3q26.2 cytoband of HGSOC [7].

The biological roles of *MECOM* and its associated proteins in HGSOC have been extensively investigated. Nanjundan et al. demonstrated that MECOM and EVI1 proteins enhance cellular proliferation, migration, and attenuate transforming growth factor-β-mediated plasminogen activator inhibitor-1 promoter activity in ovarian epithelial cells [7]. Concurrently, they identified a link between increased *MECOM* transcript levels and favorable patient outcomes, whereas elevated EVI1 transcript levels correlated with poorer survival in a cohort of stage III/IV HGSOC patients [7]. Contrarily, Jazaeri et al. did not find a significant association between EVI1 protein expression and ovarian cancer cell growth [8]. Moreover, studies have suggested that the MECOM isoform serves as a pivotal transcription factor sustaining HGSOC in vivo growth, functioning as a cofactor for paired box 8 (PAX8) and mediating a subset of PAX8's oncogenic activities [6]. Thus, the influence of *MECOM* and *EVI1* transcripts and protein isoforms on ovarian cancer cells and patient prognosis remains contested. Additionally, the tumor immune microenvironment's (TIME) impact on cancer patient outcomes, particularly regarding immune checkpoint therapy, has drawn significant attention [9–11]. Nonetheless, the potential influence of *MECOM* gene products on TIME regulation has yet to be explored.

Given *MECOM's* significance in HGSOC and the divergent findings in existing research, an in-depth investigation of the association between various transcripts and clinical prognosis in a larger cohort is warranted. This study integrates and examines different *MECOM* transcript expressions from RNA-sequencing (RNA-seq) data collated in the Genotype-Tissue Expression (GTEx) and The Cancer Genome Atlas (TCGA) databases. Furthermore, the study investigates the influence of these transcripts on patient prognosis and TIME in HGSOC using bioinformatics tools and identifies potential regulatory targets for the different protein isoforms acting as TF through Chromatin Immunoprecipitation (ChIP) RNAseq data analysis.

Materials and methods

Data sources

Transcript expression data from RNA-seq in the GTEx (https://gtexportal.org/home/) TCGA (https://portal.gdc.cancer.gov/) databases were retrieved from the "TCGA TARGET GTEx" study using the UCSC Xena Toil RNA-Seq Recompute Compendium (htxxps://xenabrowser.net/) on April 22, 2023. The RSEM TPM dataset for transcript expression was downloaded from UCSC Xena, and data specific to "Ovarian Serous Cystadenocarcinoma" of TCGA and "Ovary" tissues of GTEX were extracted. Furthermore, mRNA expression data along with corresponding clinical information (age, stage, and additional patient details) for HGSOC samples were obtained from UCSC Xena (htxxps://xenabrowser.net/datapages/). Patients with incomplete RNA-Seq data (67 cases) or lacking complete overall survival information (1 case) were excluded from the analysis. The study ultimately included 352 HGSOC cases and 88 normal samples, with clinical characteristics detailed in Supplemental Table 1 (Table S1).

Survival Analysis and Cox Regression Analysis

The optimal cutoff values for variables requiring analysis were determined using the "surv_cutpoint" function from the "survminer" R package, and uses these values to divide patients into high-expression and low-expression groups. Kaplan-Meier curves, were generated to contrast survival rates between the two expression levels. The "survival_analysis" tools within Hiplot Pro (https://hiplot.com.cn), a comprehensive service for the analysis and visualization of biomedical data, enabled the graphical representation of this data. The association between *MECOM* transcript expression and the overall survival (OS) of HGSOC patients was evaluated using the Cox proportional hazards regression model. Both univariate and multivariate analyses were conducted using the "forestplot" R package to ascertain the potential of different isoforms' expression as an independent prognostic marker for cancer patients. The multivariate analysis incorporated factors such as age, stage, tumor

grade, tumor residential, and transcript expression levels, employing the "coxph" function in R for computation. Subsequently, the "forestplot" R package yielded forest plots that clearly depicted the P values, hazard ratios (HRs), and 95% confidence intervals (CIs) for each variable under consideration.

Exploration of Immune-related signatures

The assessment of immune features and immune cell infiltration across different groups was performed using the Immuno-Oncology Biological Research (IOBR) R package [12]. The "IOBR" package aggregates 322 signature gene sets from the literature to evaluate immune suppression, exclusion, and exhaustion in the TIME, applying various evaluation algorithms and signature sets. Furthermore, six algorithms—CIBERSORT [13], ESTIMATE [14], TIMER [15], quanTIseq [16], MCP-counter [17], and EPIC [18]—were employed to determine the composition of tumor-infiltrating immune cells using expression profiles from the "TCGA-OV" cohort, functionalities integrated within the "IOBR" package. Details on data coding and analytical methodologies are provided in the Supplemental Methods section.

Web analysis

In this study, analyses were conducted on mutations, potential copy-number alterations identified through GISTIC, and structural variants of the *MECOM* gene using the cBioPortal platform (https://www.cbioportal.org/). Functions of protein isoforms were investigated via the UniProt (https://www.uniprot.org/) and NextProt (https://www.nextprot.org/) databases. The correspondence between gene mRNA transcripts and protein isoforms was determined through the Ensembl database (https://www.ensembl.org/index.html). Sequence specificity among different transcripts was compared using the BLAST database (https://blast.ncbi.nlm.nih.gov). The Clinical Proteomic Tumor Analysis Consortium (CPTAC) database (https://cprosite.ccr.cancer.gov/) was utilized to explore the correlation between protein abundance and *MECOM* gene mRNA in human HGSOC. Furthermore, the Kaplan-Meier Plotter (https://kmplot.com/analysis/), drawing data from the Gene Expression Omnibus (GEO) and TCGA databases, assessed the impact of JUN expression on the survival of patients with ovarian cancer.

ChIP-seq analysis

ChIP-Seq datasets pertaining to MECOM were retrieved from the Sequence Read Archive (SRA) database (PRJNA655844), and datasets including peak information for EVI1 were sourced from the GEO database (GSE25210). These datasets have been mapped to the human genome (version hg19). The annotation and comparison of ChIP peak were conducted using "ChIPseeker" [19], an R/Bioconductor package. Annotation packages employed included "TxDb.Hsapiens.UCSC.hg19.knownGene" and "org.Hs.eg.db" (Bioconductor). Promoters were defined as ±3 kb from the transcription start site. Functions such as "annotatePeak", "peakHeatmap", "plotAvgProf2", "plotAnnoPie", "plotAnnoBar" were utilized for visualizing the results.

RNAseq DEG analysis

Gene expression profiles of ovarian cancer cells were acquired from GEO dataset GSE25213 and SRA dataset PRJNA655836. Data analysis for identifying differentially expressed genes (DEGs) utilized the R/Bioconductor software packages limma and DESeq2 respectively. The criteria selected for visualizing DEGs on volcano plots were |log2 fold change| > 0.5 and adjusted p-value (padj) < 0.05.

Pathway enrichment analysis

Genes intersecting between ChIP-seq and RNA-seq-derived DEGs were extracted and underwent pathway enrichment analysis. Enrichment analyses for Gene Ontology (GO), Kyoto Encyclopedia of Genes and Genomes (KEGG) [20, 21], and WikiPathways were conducted utilizing the "clusterProfiler" package in R. Significant pathways related to cancer were identified using Reactome tools (https://reactome.org). GO analysis encompasses biological processes, cellular components, and molecular functions, serving as a bioinformatics approach for gene and protein annotation to elucidate characteristic biological attributes. The "simplify" function within the R package was employed to reduce redundancy in the enriched GO terms output. Directed acyclic graphs (DAGs) illustrating the hierarchical relationships among GO terms were generated using the "topGO" R package, providing a tree-like visual representation. The circos plot were performed using the OECloud tools at https://cloud.oebiotech.com.

Statistical tests

Data analysis in the study was conducted primarily using R language (version 4.2.2). The "ggplot2" package facilitated figure creation. The Wilcoxon test estimated statistical significance for quantitative data comparisons between two types. Kaplan-Meier survival analysis employed the log-rank method to determine statistical significance. Values of $p < 0.05$ were deemed statistically significant, with significance levels denoted as $^{*}p < 0.05$, $^{**}p < 0.01$, $^{***}p < 0.001$, and $^{****}p < 0.0001$.

Results

Expression of MECOM Transcripts in Normal and HGSOC

Genomic alterations in the *MECOM* locus have been implicated in various cancers, with mutations, deep deletions, structural variants, and amplifications documented (Fig. 1A). An analysis of the "TCGA PanCancer Alters Studies" within the cBioPortal database revealed a high incidence of such genomic alterations in ovarian epithelial tumors, with significant *MECOM* amplification observed in up to 30% of cases (Fig. 1A, Figure S1A). Survival analysis of 352 HGSOC patients indicated that *MECOM* gene amplification did not serve as a direct prognostic indicator for OS (Figure S1B). The human *MECOM* gene is known to produce at least twenty mRNA transcripts (Fig. 1B, Figure S1C, Table S2), with nineteen variants quantified in the "TCGA TARGET GTEx" study of UCSC Xena Toil RNA-Seq Recompute Compendium. The expression levels (log2(tpm+0.001)) of all *MECOM* transcripts in HGSOC and corresponding normal tissues were delineated through a heatmap (Fig. 1C). Out of these transcripts, six variants were identified as being expressed in over 85% of the tissues (yellow shading in Fig. 1B-C), with their expression levels in tumor tissues significantly elevated compared to normal tissues (Fig. 1D).

Different *MECOM* gene transcripts often yield proteins with variant domain compositions, thereby influencing their biological functions. The proteins isoform 1 (EVI1 isoform) and isoform 7 (MECOM isoform), derived from the *MECOM* gene, are the principal variants exerting biological functions, as indicated by UniProt and NextProt database searches. The shorter transcript ENST00000628990.2, detailed in ENSEMBL, encodes a 1051 amino acid, 145 kDa EVI1 protein isoform (UniProt ID: Q03112-1) (Table S2). A longer transcript, ENST00000494292.6, encodes a 1230 amino acid, 185 kDa MECOM protein variant (UniProt ID: Q03112-7) (Table S2). Consequently, the subsequent analysis primarily focuses on the effects of these two classical isoforms and their corresponding transcripts on HGSOC.

Association between Classical isoforms and patients' survival of HGSOC

Sequence alignment analyses via BLAST revealed that the two classical *MECOM* transcripts share an identical 3' end sequence of 4747 nucleotides, differing only at the 5' end (Fig. 2A). The longer isoform, MECOM, represents a fusion protein, wherein MDS1 exon 2 is in-frame fused with EVI1 exon 2, contributing an additional 188 amino acids to the EVI1's normal starting codon in exon 3. The EVI1 protein is characterized by two zinc-finger (ZF) DNA-binding domains, with the first containing seven ZF motifs at the amino terminus and the second comprising three ZF motifs at the carboxyl terminus (Fig. 2A). MECOM isoforms, featuring a PR domain from MDS1 at the N-terminus combined with ZF domains from EVI1, belong to the PRDM (PR/SET domain) protein family, also known as PRDM3 (Fig. 2A).

To assess the impact of expression levels of these variants on patient prognosis, patients were stratified into high- and low-expression groups using the optimal cutoff (Fig. 2B-C). Kaplan-Meier survival analysis indicated that high expression of the MECOM isoform correlated with poorer survival (Fig. 2D), whereas high expression of the EVI1 isoform was associated with improved survival (Fig. 2E). Subsequent univariate and multivariate Cox regression analyses, which included age, pathological stage, grade, and postoperative residual tumor status, confirmed that MECOM transcript expression constitutes a prognostic risk factor (HR=1.38, 95% CI: 1.03–1.86), while EVI1 transcript expression serves as a protective factor (HR=0.86, 95% CI: 0.77–0.96) (Fig. 2F-G).

The Effect of classical transcripts on TIME of HGSOC

In recent years, the TIME has garnered increased attention, with studies shifting focus from solely targeting tumor cell eradication to understanding the complex interplay within the TIME and its implications on therapeutic efficacy. Nevertheless, the potential role of *MECOM* in modulating TIME remains unexplored. Comparative analyses were conducted to examine TIME characteristics between high- and low-expression subgroups derived from two distinct MECOM transcripts. Utilizing the "IOBR" package for further TIME signature analysis, it was established that patients with high MECOM isoform expression exhibited an immunosuppressive, exclusive, and exhausted TIME (Fig. 3A-C). Such patients presented elevated levels of exhausted $CD8^+$ T cells (Fig. 3C), increased immune checkpoint signature scores (Fig. 3A), and higher presence of immunosuppressive cells, including myeloid-derived suppressor cells (MDSCs), M2-type tumor-associated macrophages (TAMs), and regulatory T cells (Tregs) (Fig. 3A-C). Conversely, patients with high expression of EVI1 isoforms displayed an opposing trend (Fig. 3D-F).

Six algorithms (CIBERSORT, TIMER, quanTIseq, EPIC, MCP-counter, and ESTIMATE) were employed to estimate immune cell abundance using the "IOBR package" (Figure S2A, Table S3). The findings indicated divergent immune cell infiltration patterns within the high-expression groups of different transcripts (Figure S2A). Notably, EPIC and quanTIseq, recognized as the most reliable deconvolution algorithms, discern various immune cell proportions through the analysis of marker gene expression levels. A differential abundance of seven or ten infiltrating immune cell types was observed in patient groups stratified by transcript expression cutoff

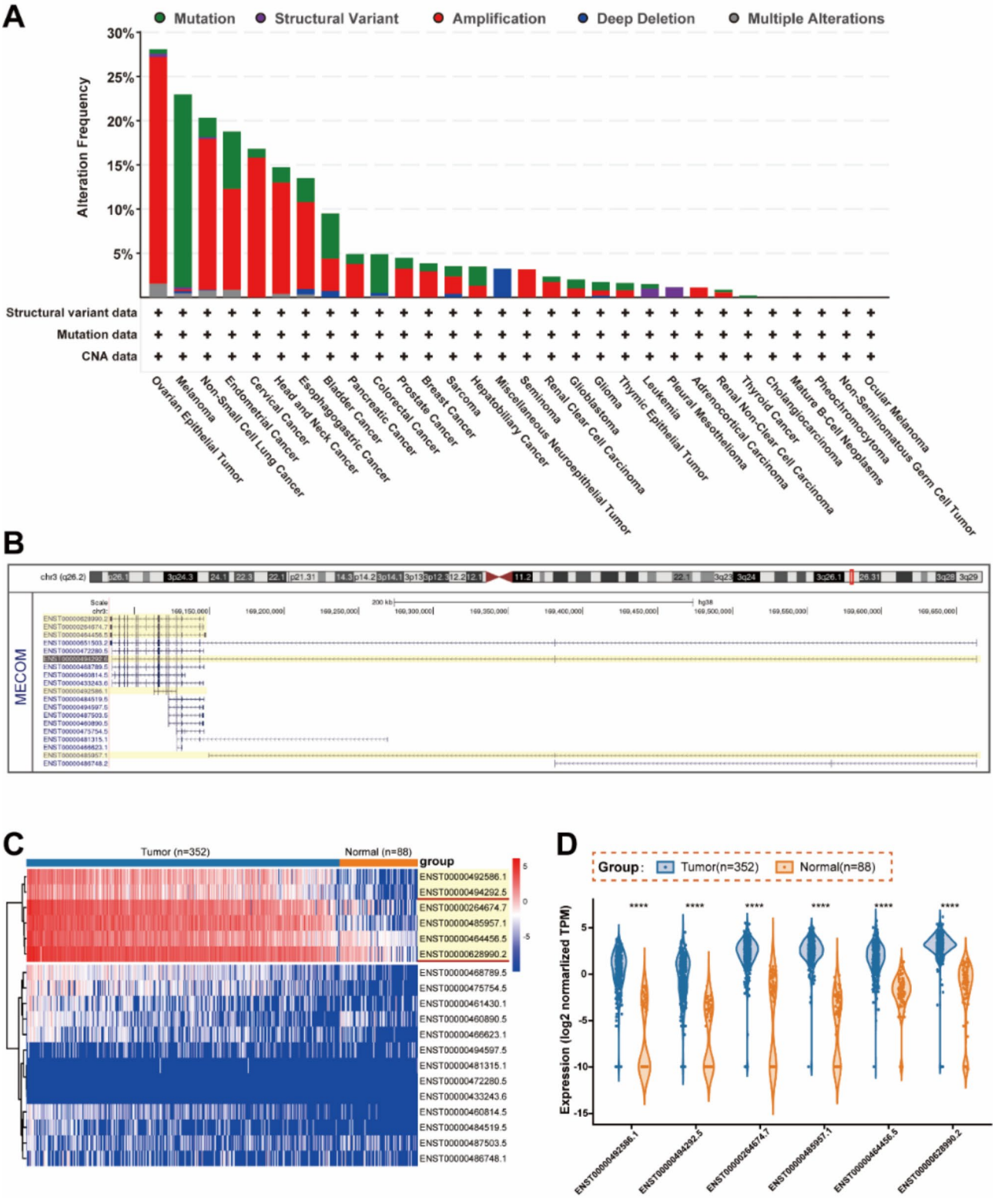

Fig. 1 *MECOM* Transcript Variability and Expression Analysis. **(A)** Genomic alterations of *MECOM* across various tumor types were examined using the "TCGA PanCancer Alters Studies" in the cBioportal database. **(B)** Nineteen gene transcripts of *MECOM*, as cataloged by UCSC, were identified. **(C)** A heatmap depicted the expression levels (log2(tpm + 0.001)) of these nineteen *MECOM* transcripts in HGSOC samples ($n = 352$) and normal ovarian tissues ($n = 88$), with six variants exhibiting expression in over 85% of tissues highlighted in yellow. **(D)** Violin plots compared the expression levels of the six predominantly expressed transcripts between ovarian cancer (blue) and normal tissues (orange)

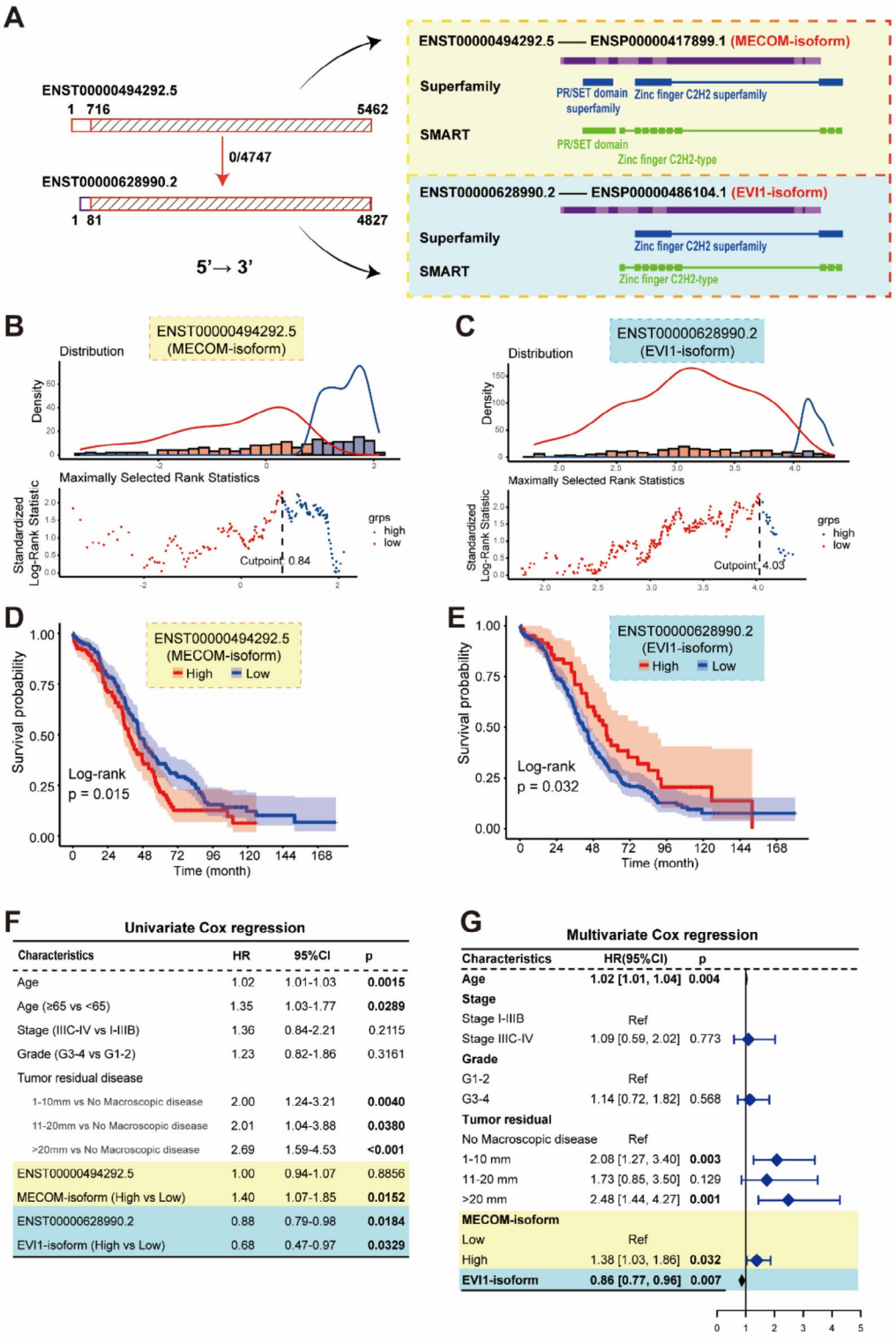

F Univariate Cox regression

Characteristics	HR	95%CI	p
Age	1.02	1.01-1.03	**0.0015**
Age (≥65 vs <65)	1.35	1.03-1.77	**0.0289**
Stage (IIIC-IV vs I-IIIB)	1.36	0.84-2.21	0.2115
Grade (G3-4 vs G1-2)	1.23	0.82-1.86	0.3161
Tumor residual disease			
1-10mm vs No Macroscopic disease	2.00	1.24-3.21	**0.0040**
11-20mm vs No Macroscopic disease	2.01	1.04-3.88	**0.0380**
>20mm vs No Macroscopic disease	2.69	1.59-4.53	**<0.001**
ENST00000494292.5	1.00	0.94-1.07	0.8856
MECOM-isoform (High vs Low)	1.40	1.07-1.85	**0.0152**
ENST00000628990.2	0.88	0.79-0.98	**0.0184**
EVI1-isoform (High vs Low)	0.68	0.47-0.97	**0.0329**

G Multivariate Cox regression

Characteristics	HR(95%CI)	p
Age	**1.02 [1.01, 1.04]**	**0.004**
Stage		
Stage I-IIIB	Ref	
Stage IIIC-IV	1.09 [0.59, 2.02]	0.773
Grade		
G1-2	Ref	
G3-4	1.14 [0.72, 1.82]	0.568
Tumor residual		
No Macroscopic disease	Ref	
1-10 mm	2.08 [1.27, 3.40]	**0.003**
11-20 mm	1.73 [0.85, 3.50]	0.129
>20 mm	2.48 [1.44, 4.27]	**0.001**
MECOM-isoform		
Low	Ref	
High	1.38 [1.03, 1.86]	**0.032**
EVI1-isoform	**0.86 [0.77, 0.96]**	**0.007**

Fig. 2 *MECOM* Classical Transcripts and HGSOC Patient Survival Prognosis. **(A)** Schematic representations of two classic *MECOM* transcripts and their protein isoforms domains were presented. **(B-C)** Optimal cutoff values were determined for ENST000000494292.6 (B) and ENST000000628990.2 (C). **(D-E)** Kaplan-Meier survival curves, using the log-rank test, evaluated the association between the expression of MECOM-isoform (D) or EVI1-isoform (E) and OS in HGSOC patients. **(F)** Univariate COX regression analysis was conducted considering clinical features and the expression levels of two classical *MECOM* transcripts. **(G)** Multivariate COX regression analysis and forest plots incorporated clinical features and expression levels of these transcripts

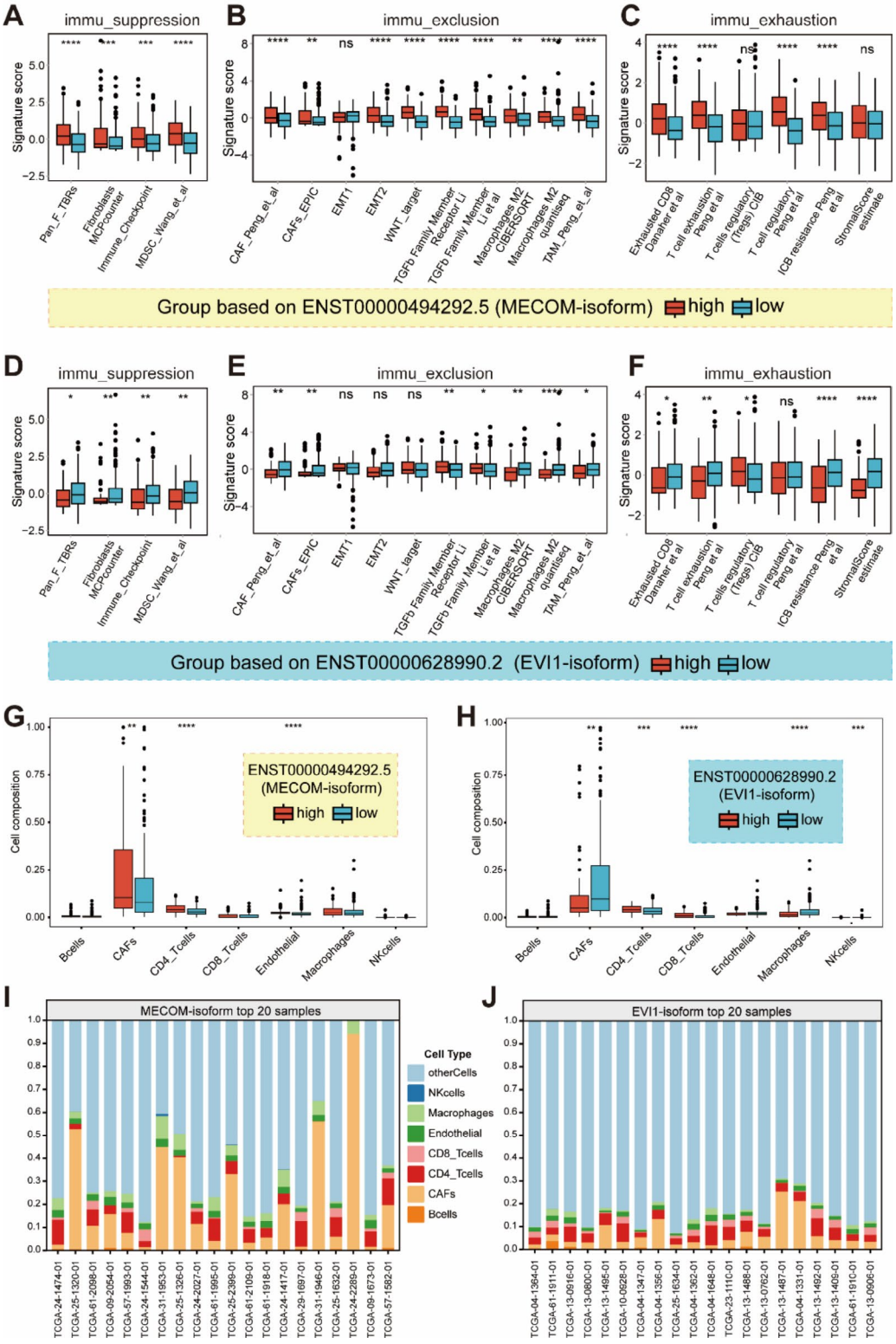

Fig. 3 Classical *MECOM* Transcripts Correlation with TIME in HGSOC. **(A-C)** Comparison of immune suppression **(A)**, exclusion **(B)**, and exhaustion **(C)** features between two subgroups of MECOM-isoform. **(D-F)** These comparisons were similarly made for subgroups based on EVI1-isoform expression. **(G-H)** The abundance of various infiltrating cells was contrasted between the high- and low-expression groups for MECOM-isoform **(G)** and EVI1-isoform **(H)**, respectively. **(I-J)** Stacked bar plots derived from the EPIC deconvolution algorithm displayed cell type proportions for the top 20 patients by expression level of MECOM-isoform **(I)** and EVI1-isoform **(J)** in the HGSOC samples

values (Fig. 3G-H, Figure S2B-C). Specifically, the high-expression group for MECOM isoforms was characterized by a significant increase in cancer-associated fibroblasts (CAFs), M2 TAMs, and Tregs ($p<0.05$) (Fig. 3G, Figure S2B). In contrast, high-expression groups for EVI1 isoforms were associated with a greater proportion of $CD8^+$ T cells and reduced levels of CAFs and M2 TAMs ($p<0.05$) (Fig. 3H, Figure S2C). To illustrate the immune cell composition within the tumor microenvironment (TME), the top 20 patients with the highest expression levels of the two classical transcripts were selected, highlighting the cell abundance variation (Fig. 3I-J). Results demonstrated a significant increase in CAFs among patients with high MECOM transcript expression (Fig. 3I-J), possibly explaining why such transcript levels are considered a risk factor for patient prognosis. CAFs are implicated in extracellular matrix (ECM) production, tumor growth support, angiogenesis, and chemoresistance. In our cohorts, patients with high CAF abundance exhibited worse prognoses (Figure S2D-E). It was thus hypothesized that the differential impact on prognosis could be ascribed to the varying association between *MECOM* transcript expressions and the immune microenvironment.

Potential targets of MECOM Isoforms as TF in HGSOC

In prior results, the expression levels of two classical *MECOM* transcripts were found to differentially impact the prognosis of HGSOC patients. These transcripts encode proteins of varying lengths, yet both encompass the canonical ZF domains capable of DNA binding and function as TF that modulate gene expression (Fig. 2A). Analysis of ChIP-Seq data from OVCAR3 ovarian cancer cells was performed to identify targets and signaling pathways regulated by MECOM that contribute to ovarian cancer malignancy. Remarkably, 838 of 7663 (10.94%) and 825 of 7642 (10.80%) peaks were discerned within promoter regions (Fig. 4A, Table S4). Investigation into the peak distribution and binding affinity around the transcription start site (TSS) revealed localized binding proximal to the TSS with high reproducibility in both samples (Fig. 4B, Figure S3A). After deduplication, these peaks corresponded to 780 and 771 distinct genes, with an overlap of 756 common genes (Fig. 4C).

Subsequent differential gene expression analysis from RNA-seq data of five ovarian cancer cell lines (COV318, IGROV1, Kuramochi, OVISE, and OVCAR3) following MECOM knockdown identified 4188 DEGs with an adjusted p-value <0.05 and an absolute log2 fold change >0.5 in any model (Figure S3 B - G, Table S4). The heatmap displayed 16 DEGs consistent across the five cell lines (Figure S3H). To pinpoint potential direct transcriptional targets of MECOM isoforms, an intersection of MECOM-bound genes with DEGs across five cell lines was conducted (Fig. 4D), revealing 89 shared genes, with their log2 fold changes depicted in a heatmap (Fig. 4E). Gene function annotations and pathway involvement were cataloged using the GO and pathway databases (KEGG, Reactome, Wikipathways) (Table S4), with an adjusted p-value (q-value) threshold of 0.10 for significant gene set enrichment. GO analysis identified five highly overrepresented categories among the direct target genes of MECOM isoforms: response to auditory stimulus, cellular response to steroid hormone stimulus, response to mechanical stimulus, detection of external stimulus, and detection of abiotic stimulus (Figure S4A). Pathway enrichment analysis highlighted significant gene involvement in the CLEC7A/inflammasome pathway, regulation of NPAS4 gene expression, and interleukin-1 processing, among others (Figure S4A-B). Notably, IL1B emerged as a gene with the extensive functional roles across various pathways (Figure S4B). In the cancer context, IL-1β exerts diverse effects on immune cells, angiogenesis, proliferation, migration, and metastasis of cancer cells. Additionally, MECOM isoforms likely regulate other key genes (such as GPR87, LY6K, TDO2, and FOXP2, Fig. 4E) that influence cytokine/chemokine production, immune checkpoint expression, and metabolic reprogramming, thereby modulating the function of immunosuppressive cells and cancer-associated fibroblasts (CAFs). Consequently, the deleterious impact of this variant on patient prognosis may be mediated through the regulation of these molecules and their corresponding pathways, with infiltration of CAFs and immunosuppressive cells are also one of the manifestations.

Potential targets of EVI1 isoforms as TF in HGSOC

To elucidate the targets and signaling pathways regulated by EVI1 in ovarian cancer, ChIP-seq and RNA-seq data from SKOV3 ovarian cells were examined. Analysis revealed that 4390 of 12,864 (34.12%) EVI1-associated peaks localized to promoter regions (Fig. 5A, Table S5). The distribution of distances between EVI1 ChIP peaks and adjacent genes was depicted in Fig. 5B. Subsequent analysis of DEGs in SKOV3 cells with EVI1 knockdown identified 116 upregulated and 119 downregulated genes, meeting the threshold of an adjusted p-value <0.05 and absolute log2 fold change >0.5 (Fig. 5C, Table S5). Integration of ChIP-Seq and DEGs yielded 50 putative EVI1 target genes (Fig. 5D-E). Gene functions and pathways were annotated using GO and Pathway databases, with redundancy in enriched GO terms minimized using the `simplify` function. Molecular function analysis overrepresented four predominant categories: protein tyrosine/threonine phosphatase activity, cell-cell adhesion mediator activity, sulfur compound transmembrane transporter activity, and MAP kinase tyrosine/serine/threonine phosphatase activity (Fig. 5F, Table S5). Hierarchical

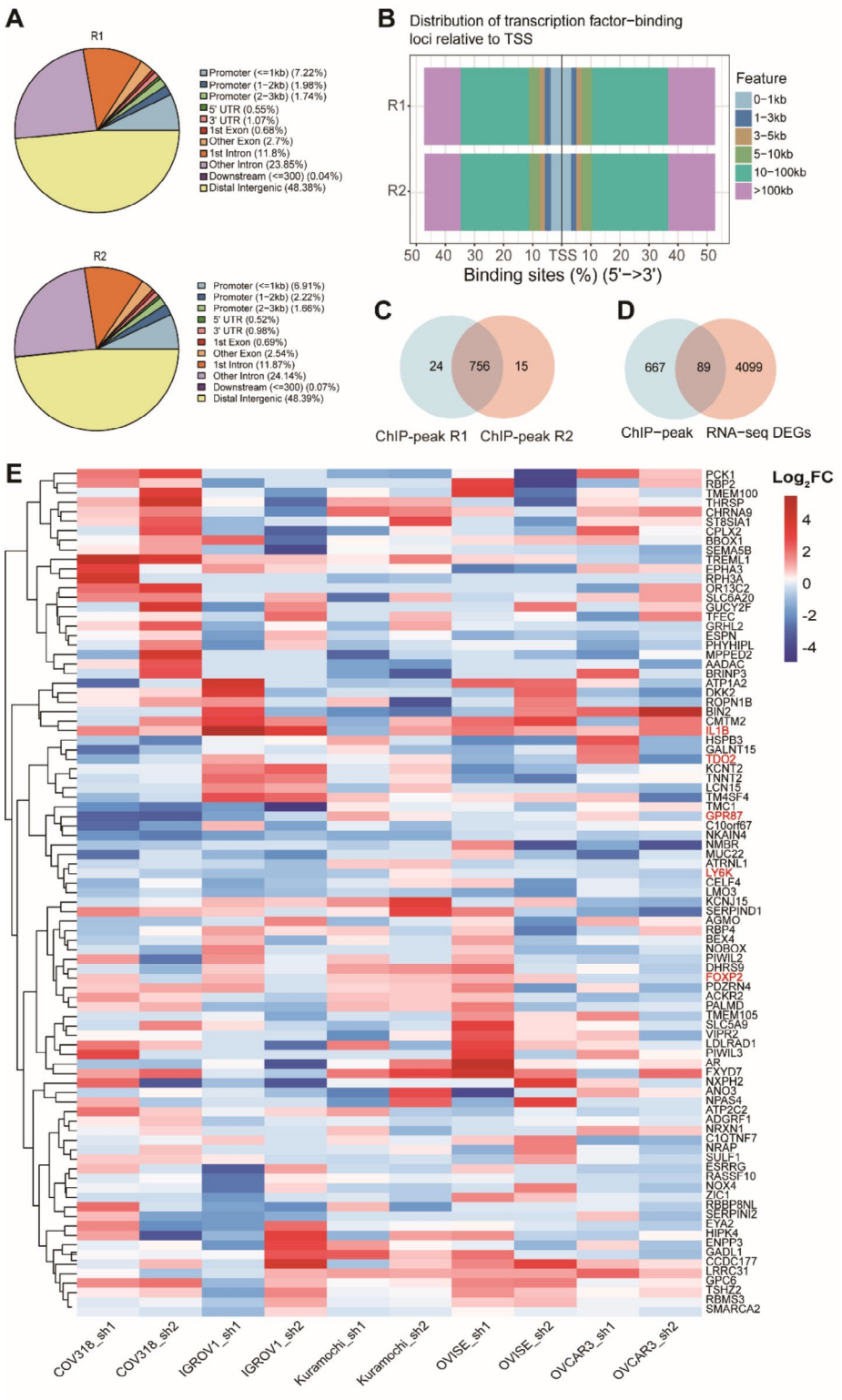

Fig. 4 Regulatory Targets of MECOM Isoforms in HGSOC Explored. **(A)** The MECOM ChIP-Seq (two replicates: R1 and R2) peak distribution pattern was analyzed in OVCAR3 cells. A total of 838/7663 (10.94%) or 825/7642 (10.80%) peaks were located at the promoter region of downstream genes. **(B)** The distribution and binding strength of peak in the upstream and downstream of TSS. **(C)** A venn diagram illustrated 756 genes shared between two ChIP-Seq replicates. **(D)** A venn diagram between 756 genes from ChIP-Seq and 4188 DEGs from transcriptome data showing 89 predicted MECOM targets. **(E)** A heatmap showed the log2fold changes in mRNA expression of the 89 target genes

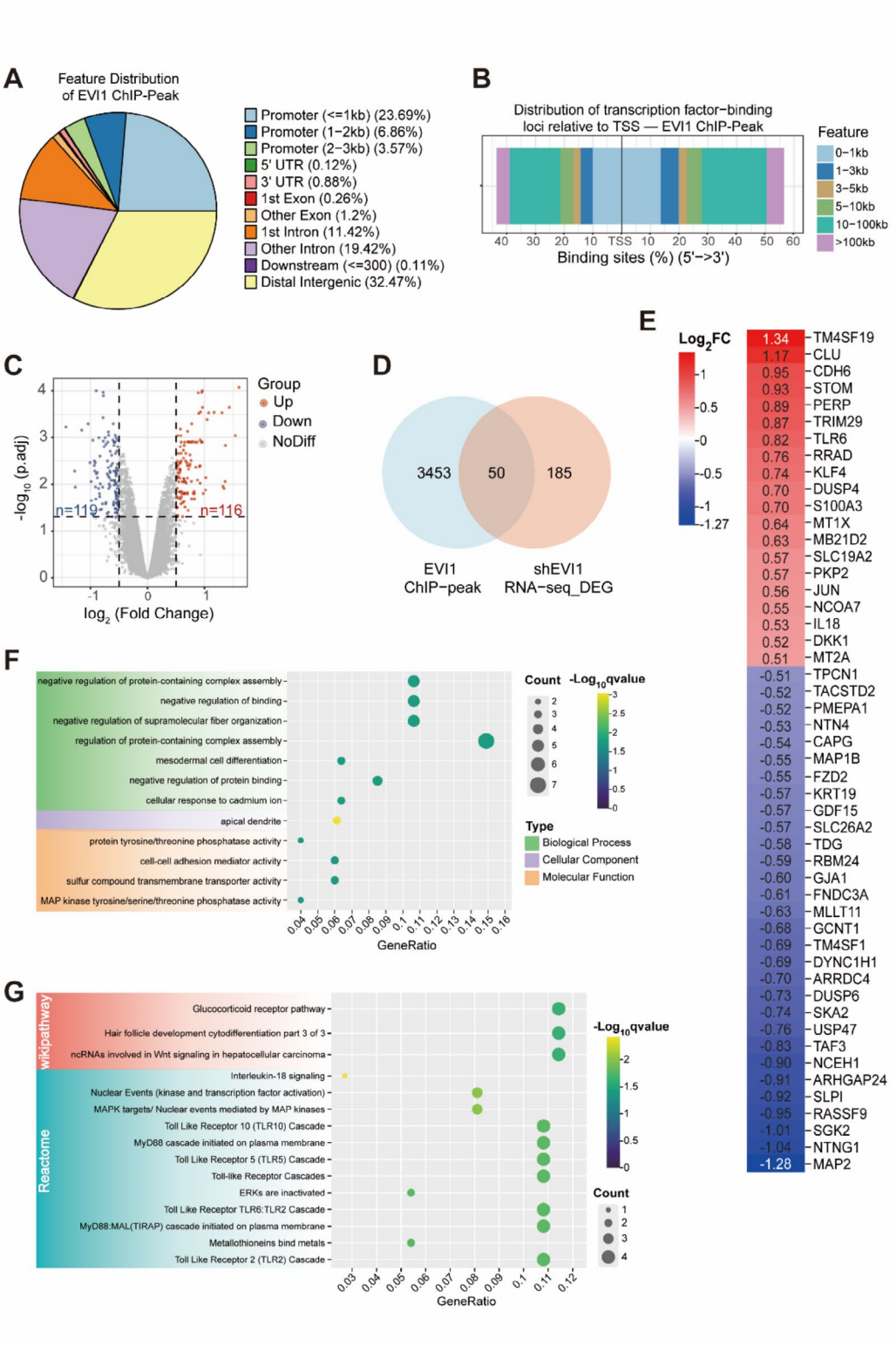

Fig. 5 Potential EVI1 Isoform Regulatory Targets in HGSOC Investigated. **(A)** The EVI1 ChIP-Seq peak distribution pattern in SKOV3 cells was analyzed, with 4390/12,864 (34.12%) of peaks located at promoters of downstream genes. **(B)** Peak distribution and binding intensities were examined around the TSS. **(C)** A volcano plot displayed DEGs following EVI1 knockdown in SKOV3 cells, highlighting significantly up- and down-regulated genes (padj < 0.05 and |log2foldchange| > 0.5). **(D)** Integration of ChIP-Seq and RNA-Seq data identified 50 potential EVI1 targets. **(E)** A heatmap depicted the log2fold changes in mRNA expression of the 50 EVI1 target genes. **(F-G)** Enrichment analyses of the GO terms **(F)** and pathways **(G)** for the 50 target genes were conducted

relationships among GO terms were visualized using DAGs generated by the bioconductor package "TopGO" (Figure S5A-B). Pathway enrichment analysis demonstrated significant gene enrichment in nuclear events (kinase and transcription factor activation), MAPK targets/ nuclear events mediated by MAP kinases, ERKs are inactivated, and Toll Like Receptor 2/5/10 (TLR2/5/10) Cascade (Fig. 5G). Further, genes involved in various pathways were identified, with JUN emerging as the most functionally diverse (Figure S6A). Concordantly, elevated JUN expression was associated with poor prognosis in ovarian cancer patients (Figure S6B-C). This analysis indicates that EVI1 may confer a protective effect by diminishing JUN protein expression or by modulating its DNA binding to downstream gene targets.

Discussion

MECOM, a pivotal TF in HGSOC [22], produces numerous gene products. While the involvement of *MECOM* in HGSOC pathogenesis has been investigated, the findings remain inconsistent. This study investigates the association between two key *MECOM* gene products, prognosis, and the TIME signature in a large HGSOC cohort. Our analysis demonstrated that elevated MECOM transcript levels were associated with poor survival in HGSOC patients, potentially by modulating CAFs and immunosuppressive cells such as MDSCs, M2 TAMs, and Tregs. In contrast, increased EVI1 transcript levels correlated with better survival, potentially by influencing $CD8^+$ T cells, reducing JUN protein expression, or altering its DNA binding to downstream genes.

High somatic copy number alterations (CNA) frequency is a hallmark of HGSOC [3, 23]. The 3q26 region, frequently amplified in ovarian cancers, contains the *MECOM* gene [5, 24, 25]. This study analyzed CNAs in a substantial TCGA cohort ($n=1691$), identifying *MECOM* amplification in roughly 30% of HGSOC samples. Additionally, elevated *MECOM* gene transcripts were noted in HGSOC compared to normal tissues. Nanjundan et al. designed several qPCR probes to assess the level of EVI1, MDS1, and the fusion transcript *MECOM*. They found *MECOM* and *EVI1* exon III (represent *EVI1+MECOM*) RNA levels are increased up to 540- and 125-fold in the majority (98% and 83%) of ovarian cancers, respectively [7]. In addition, they found that the increases in EVI1 DNA copy number and MDS1/EVI1 transcripts are associated with improved patient outcomes [7]. However, the present study found no impact of *MECOM* gene amplification on patient survival.

Gene function is typically mediated by protein products synthesized via mRNA translation. Analysis of the CPTAC database revealed a positive correlation between the abundance of *MECOM* gene proteins and their mRNA in human ovarian cancer, with a correlation coefficient of 0.7489. However, distinct protein molecules encoded by a single gene may exhibit diverse functions [26]. Thus, investigating the molecular mechanisms underlying disease pathogenesis and identifying potential drug target proteins at the level of splice variant isoforms are of paramount importance [27]. Our findings confirmed that transcripts corresponding to MECOM isoforms were predictors of poor patient outcomes, echoing findings in lung squamous cell carcinoma [28]. It was observed that forced expression of MECOM isoforms in cell lines promoted cancer stem cell properties [28]. Our research has preliminarily revealed that the MECOM isoforms regulate genes such as IL1B, GPR87, TDO2, LY6K, and FOXP2, which have been closely linked to pathway activation, metabolic reprogramming, and immune checkpoint expression in prior studies [29–33]. In ovarian cancer, the MECOM isoforms may promote immunosuppression and remodeling of the tumor microenvironment through these mechanisms, ultimately driving tumor growth and immune evasion. This may provide a potential explanation for the association between MECOM transcripts and poor prognosis.

For another classic variant, numerous studies have indicated that EVI1, an oncogenic TF, is overexpressed in myeloid malignancies and several solid tumors, including prostate and colon cancer, contributing to disease progression and an aggressive phenotype [34–36]. In HGSOC, research has suggested that EVI1 targets the PDZ-binding kinase to promote metastasis and confer cisplatin resistance through the induction of autophagy [37]. Furthermore, EVI1 has been shown to regulate estrogen signaling by directly activating transcription of estrogen receptor 1, promoting cell proliferation and invasion in vitro as well as tumor growth in xenograft models [38]. However, our study demonstrated that the presence of transcripts corresponding to the EVI1 isoforms is linked to a better prognosis in HGSOC patients. Additionally, analyses of the TIME revealed that patients with high levels of these transcripts exhibited an increased proportion of $CD4^+$ T and $CD8^+$T cells, and a decreased proportion of CAFs and M2 TAMs, supporting the prognostic implications of earlier findings. In the study of Bard Chapeau EA et al., they showed that more than 25% of EVI1-occupied genes contain linked EVI1 and activator protein-1 complex DNA binding sites, and they indicate that EVI1 synergizes with FOS in invasive tumors [39]. JUN and FOS are components of the activator protein-1 (AP-1), which plays a crucial role in multiple cancer-related signaling pathways [40]. Our analysis suggests that EVI1 may have a protective role in patients by downregulating the expression of the JUN protein or altering its DNA binding activity to downstream genes. Consistent with these findings, Jazaeri AA et al. observed that EVI1 inhibited the growth of 293T and ES2 cells, and selective knockdown of EVI1 isoforms did not impact cell proliferation, cisplatin-induced apoptosis, or γ-H2AX levels in ovarian cancer cells

[8]. Furthermore, they found that transcripts of EVI1 were nearly ubiquitously expressed in ovarian cancer samples and benign tissues thought to be the origin of these malignancies, such as the normal ovaries and fallopian tube fimbriae [8]. In contrast, the protein levels of EVI1 isoforms were undetectable in normal ovarian tissues, displaying similar patterns between serous ovarian cancer samples, fallopian tube fimbriae, and benign neoplasms [8]. This suggests that the expression of EVI1 in serous cancers may reflect the histopathological tissue of origin rather than represent an oncogenic event.

Our research is subject to certain limitations. Primarily, the analyses were founded upon the mRNA expression levels of various *MECOM* transcripts. While database analyses have demonstrated a robust correlation between the mRNA and protein expression of this gene, the levels of individual transcripts may not precisely reflect the protein isoform's expression or functional activities. RNA editing, translation efficiency, post-translational modifications, and protein localization can influence the functionality of distinct protein isoforms within cancerous contexts. Presently, a comprehensive protein database cataloging the expression levels of different protein isoforms from identical genes does not exist; however, such a resource might be developed in the future, leveraging advancements in sequencing technologies and the accumulation of research data. In summary, the study advances our understanding of *MECOM* gene products in HGSOC, highlighting their complex roles in prognosis and the TIME, while acknowledging the need for further experimental validation.

Conclusion

The diverse protein isoforms derived from *MECOM* exhibit distinct impacts on the survival and tumorigenesis in HGSOC patients via specific mechanisms. Investigating the molecular mechanism of disease pathogenesis and searching for drug target proteins at the level of splicing homologous isoforms are critical.

Supplementary Information

The online version contains supplementary material available at https://doi.org/10.1186/s13048-024-01522-0.

Supplementary Material 1

Supplementary Material 2

Supplementary Material 3

Supplementary Material 4

Supplementary Material 5

Supplementary Material 6

Supplementary Material 7

Acknowledgements

The authors acknowledge Shanghai Tengyun Biotechnology Co., Ltd. for the development of the Hiplot Pro platform (https://hiplot.com.cn/), along with the provision of technical assistance and valuable tools for data analysis and visualization.

Author contributions

Conceptualization, N. L. and J. R.; methodology, N. L.; software, N. L. and S. B.; validation, N. L.; data curation, M. C., X. W. and Z. F.; writing—original draft preparation, N. L., S. B. and J. R.; writing —review and editing, M. C., X. W., Z. F., Y. G., B. H., W. M., X. Z., F. H., Wa. L., We. L., and F. W.; visualization, N. L.; funding acquisition, J. R. and Y. G. All authors have read and agreed to the published version of the manuscript.

Funding

This manuscript was supported by several grants. The National Natural Science Foundation of China (Juan Ren, 82473252). The Scientific and Technological Research Foundation of Shaan'xi Province, Key Research and Development Project, General project (Juan Ren, 2023-YBSF-666). Additional support came from the Shaanxi Provincial Key Research and Development Plan Project (Key support projects Category A) (Juan Ren, 2021A011). The Basic and Clinical Integration Innovation Project of Xi'an Jiao tong University also contributed to funding (Juan Ren, YXJLRH2022006; Ying Gao, YXJLRH 2022004). Lastly, the Nanjing Tianqing Scientific Research Fund of First Affliated Hospital of Xi'an Jiaotong University provided support (Juan Ren, 2023, TQ202205).

Data availability

The datasets underpinning the conclusions drawn in this article are incorporated within the text. Transcript expression RNAseq data were obtained from the UCSC Xena Toil RNA-Seq Recompute Compendium as part of the "TCGA TARGET GTEx" study (https://xenabrowser.net/). Additional datasets created and/or analysed during the course of this study can be accessed through the specified repository URLs: the National Center for Biotechnology Information's Gene Expression Omnibus (https://www.ncbi.nlm.nih.gov/geo/), Sequence Read Archive (https://www.ncbi.nlm.nih.gov/sra), alongside databases like cBioPortal for Cancer Genomics (https://www.cbioportal.org/), UniProt (https://www.uniprot.org/), neXtProt (https://www.nextprot.org/), Ensembl Genome Browser (https://www.ensembl.org/index.html), the Cancer Proteome Atlas (https://prosite.ccr.cancer.gov/), BLAST (https://blast.ncbi.nlm.nih.gov), and KM Plotter for survival analysis (https://kmplot.com/analysis/)

Declarations

Ethics approval and consent to participate

Not applicable.

Consent for publication

Not applicable.

Competing interests

The authors declare no competing interests.

Received: 8 July 2024 / Accepted: 24 September 2024
Published online: 19 October 2024

References

1. Kandalaft L, Dangaj Laniti D, Coukos G. Immunobiology of high-grade serous ovarian cancer: lessons for clinical translation. Nat Rev Cancer. 2022;22(11):640–56.
2. Labidi-Galy SI, Papp E, Hallberg D, Niknafs N, Adleff V, Noe M, et al. High grade serous ovarian carcinomas originate in the fallopian tube. Nat Commun. 2017;8(1):1093.
3. Network CGAR. Integrated genomic analyses of ovarian carcinoma. Nature. 2011;474(7353):609–15.
4. Nameki R, Chang H, Reddy J, Corona RI, Lawrenson K. Transcription factors in epithelial ovarian cancer: histotype-specific drivers and novel therapeutic targets. Pharmacol Ther. 2021;220:107722.

5. Ballabio S, Craparotta I, Paracchini L, Mannarino L, Corso S, Pezzotta MG, et al. Multisite analysis of high-grade serous epithelial ovarian cancers identifies genomic regions of focal and recurrent copy number alteration in 3q26.2 and 8q24.3. Int J Cancer. 2019;145(10):2670–81.
6. Bleu M, Mermet-Meillon F, Apfel V, Barys L, Holzer L, Bachmann Salvy M, et al. PAX8 and MECOM are interaction partners driving ovarian cancer. Nat Commun. 2021;12(1):2442.
7. Nanjundan M, Nakayama Y, Cheng K, Lahad J, Liu J, Lu K, et al. Amplification of MDS1/EVI1 and EVI1, located in the 3q26.2 amplicon, is associated with favorable patient prognosis in ovarian cancer. Cancer Res. 2007;67(7):3074–84.
8. Jazaeri A, Ferriss J, Bryant J, Dalton M, Dutta A. Evaluation of EVI1 and EVI1s (Delta324) as potential therapeutic targets in ovarian cancer. Gynecol Oncol. 2010;118(2):189–95.
9. Pagès F, Galon J, Dieu-Nosjean MC, Tartour E, Sautès-Fridman C, Fridman WH. Immune infiltration in human tumors: a prognostic factor that should not be ignored. Oncogene. 2010;29(8):1093–102.
10. Odunsi K. Immunotherapy in ovarian cancer. Ann Oncol. 2017;28(suppl8):viii1–7.
11. Fucikova J, Coosemans A, Orsulic S, Cibula D, Vergote I, Galluzzi L et al. Immunological configuration of ovarian carcinoma: features and impact on disease outcome. J Immunother Cancer. 2021;9(10).
12. Zeng D, Ye Z, Shen R, Yu G, Wu J, Xiong Y, et al. IOBR: Multi-omics Immuno-Oncology Biological Research to Decode Tumor Microenvironment and signatures. Front Immunol. 2021;12:687975.
13. Newman AM, Liu CL, Green MR, Gentles AJ, Feng W, Xu Y, et al. Robust enumeration of cell subsets from tissue expression profiles. Nat Methods. 2015;12(5):453–57.
14. Yoshihara K, Shahmoradgoli M, Martínez E, Vegesna R, Kim H, Torres-Garcia W, et al. Inferring tumour purity and stromal and immune cell admixture from expression data. Nat Commun. 2013;4:2612.
15. Li T, Fu J, Zeng Z, Cohen D, Li J, Chen Q, et al. TIMER2.0 for analysis of tumor-infiltrating immune cells. Nucleic Acids Res. 2020;48(W1):W509–14.
16. Finotello F, Mayer C, Plattner C, Laschober G, Rieder D, Hackl H, et al. Molecular and pharmacological modulators of the tumor immune contexture revealed by deconvolution of RNA-seq data. Genome Med. 2019;11(1):34.
17. Becht E, Giraldo NA, Lacroix L, Buttard B, Elarouci N, Petitprez F, et al. Estimating the population abundance of tissue-infiltrating immune and stromal cell populations using gene expression. Genome Biol. 2016;17(1):218.
18. Racle J, de Jonge K, Baumgaertner P, Speiser DE, Gfeller D. Simultaneous enumeration of cancer and immune cell types from bulk tumor gene expression data. ELife. 2017;6:e26476.
19. Yu G, Wang L-G, He Q-Y. ChIPseeker: an R/Bioconductor package for ChIP peak annotation. Comparison Visualization Bioinf. 2015;31(14):2382–83.
20. Kanehisa M, Goto S. KEGG: kyoto encyclopedia of genes and genomes. Nucleic Acids Res. 2000;28(1):27–30.
21. Kanehisa M, Furumichi M, Sato Y, Kawashima M, Ishiguro-Watanabe M. KEGG for taxonomy-based analysis of pathways and genomes. Nucleic Acids Res. 2023;51(D1):D587–92.
22. Reddy J, Fonseca M, Corona R, Nameki R, Segato Dezem F, Klein I, et al. Predicting master transcription factors from pan-cancer expression data. Sci Adv. 2021;7(48):eabf6123.
23. Gorringe KL, Jacobs S, Thompson ER, Sridhar A, Qiu W, Choong DYH, et al. High-resolution single nucleotide polymorphism array analysis of epithelial ovarian cancer reveals numerous microdeletions and amplifications. Clin Cancer Res. 2007;13(16):4731–39.
24. Hagerstrand D, Tong A, Schumacher SE, Ilic N, Shen RR, Cheung HW, et al. Systematic interrogation of 3q26 identifies TLOC1 and SKIL as cancer drivers. Cancer Discov. 2013;3(9):1044–57.
25. Gray JW, Suzuki S, Kuo W-L, Polikoff D, Deavers M, Smith-McCune K et al. Specific keynote: genome copy number abnormalities in ovarian cancer. Gynecol Oncol. 2003;88(1 Pt 2).
26. Smith LM, Kelleher NL. Proteoform: a single term describing protein complexity. Nat Methods. 2013;10(3):186–87.
27. Yang X, Coulombe-Huntington J, Kang S, Sheynkman GM, Hao T, Richardson A, et al. Widespread Expansion Protein Interact Capabilities Altern Splicing Cell. 2016;164(4):805–17.
28. Ma Y, Kang B, Li S, Xie G, Bi J, Li F, et al. CRISPR-mediated MECOM depletion retards tumor growth by reducing cancer stem cell properties in lung squamous cell carcinoma. Mol Ther. 2022;30(11):3341–57.
29. Das S, Shapiro B, Vucic EA, Vogt S, Bar-Sagi D. Tumor cell-derived IL1β promotes Desmoplasia and Immune suppression in pancreatic Cancer. Cancer Res. 2020;80(5):1088–101.
30. Bai R, Zhang J, He F, Li Y, Dai P, Huang Z, et al. GPR87 promotes tumor cell invasion and mediates the immunogenomic landscape of lung adenocarcinoma. Commun Biol. 2022;5(1):663.
31. Jiang J, Yu C, Guo X, Zhang H, Tian S, Cai K, et al. G protein-coupled receptor GPR87 promotes the expansion of PDA stem cells through activating JAK2/STAT3. Mol Ther Oncolytics. 2020;17:384–93.
32. Kim J-H, Hwang J, Jung JH, Lee H-J, Lee DY, Kim S-H. Molecular networks of FOXP family: dual biologic functions, interplay with other molecules and clinical implications in cancer progression. Mol Cancer. 2019;18(1):180.
33. AlHossiny M, Luo L, Frazier WR, Steiner N, Gusev Y, Kallakury B, et al. Ly6E/K signaling to TGFβ promotes breast Cancer Progression, Immune escape, and Drug Resistance. Cancer Res. 2016;76(11):3376–86.
34. Birdwell C, Fiskus W, Kadia T, DiNardo C, Mill C, Bhalla K. EVI1 dysregulation: impact on biology and therapy of myeloid malignancies. Blood cancer J. 2021;11(3):64.
35. Liang B, Wang J. EVI1 in leukemia and solid tumors. Cancers (Basel). 2020;12(9).
36. Queisser A, Hagedorn S, Wang H, Schaefer T, Konantz M, Alavi S, et al. Ecotropic viral integration site 1, a novel oncogene in prostate cancer. Oncogene. 2017;36(11):1573–84.
37. Ma H, Li Y, Wang X, Wu H, Qi G, Li R, et al. PBK, targeted by EVI1, promotes metastasis and confers cisplatin resistance through inducing autophagy in high-grade serous ovarian carcinoma. Cell Death Dis. 2019;10(3):166.
38. Wang Z, Li Y, Wang N, Li P, Kong B, Liu Z. EVI1 overexpression promotes ovarian cancer progression by regulating estrogen signaling. Mol Cell Endocrinol. 2021;534:111367.
39. Bard-Chapeau EA, Jeyakani J, Kok CH, Muller J, Chua BQ, Gunaratne J, et al. Ecotopic viral integration site 1 (EVI1) regulates multiple cellular processes important for cancer and is a synergistic partner for FOS protein in invasive tumors. Proc Natl Acad Sci U S A. 2012;109(6):2168–73.
40. Bejjani F, Evanno E, Zibara K, Piechaczyk M, Jariel-Encontre I. The AP-1 transcriptional complex: local switch or remote command? Biochim Biophys Acta Rev Cancer. 2019;1872(1):11–23.

Publisher's note